# Frayed Wires: A Thermally Stable Form of DNA with Two Distinct Structural Domains†

Ekaterina Protozanova and Robert B. Macgregor, Jr.*

*Faculty of Pharmacy, University of Toronto, Toronto, Ontario, Canada*

*Received February 20, 1996; Revised Manuscript Received August 21, 1996*[⊗]

ABSTRACT: In aqueous solutions containing mono- and divalent cations, the oligodeoxyribonucleotide $d(A_{15}G_{15})$ readily self-assembles into high-molecular weight species that resolve as discrete bands on native and denaturing electrophoresis gels. The complexes consist of an integer number of strands of $d(A_{15}G_{15})$, the number of strands range from one (the monomer) to greater than nine. The complexes form within a few minutes even at low concentrations (2 $\mu$M strands) of $d(A_{15}G_{15})$. The relative concentration of species is determined by the solvent conditions. The complexes are resistant to standard denaturation conditions, 50% formamide heated to 95 °C for 2 min followed by electrophoresis in 7 M urea at 55 °C. In the proposed model for the oligomers and polymers of $d(A_{15}G_{15})$, several molecules of $d(A_{15}G_{15})$ interact via a stem of tetraplex structure formed by the guanine residues. The 15 guanine residues in the stem account for its high stability. The 5′ end adenines form single-stranded arms that are displaced from the guanine-containing stem. The arms can participate in the formation of Watson−Crick base pairs with $dT_{10}$ and other partially complementary oligodeoxyribonucleotides such as $d(CT_{15})$. Engagement of the arms in interactions with other strands does not affect the distribution of the species between different conformations. On the other hand, the addition of the fully complementary oligodeoxyribonucleotide $d(C_{15}T_{15})$ to the polymer leads to the disappearance of the high-molecular weight complexes and results in the formation of a canonical Watson−Crick base-paired duplex. The type and concentration of the cation present in solution determine which conformation $d(A_{15}G_{15})$ will adopt. Divalent cations at millimolar concentrations lead to the formation of the polymer, while the presence of the monovalent cations stabilizes lower-molecular weight complexes consisting of two to six strands of $d(A_{15}G_{15})$.

DNA can adopt a number of so-called noncanonical structures such as parallel duplexes and triple-stranded and quadruple-stranded helices. Guanine-rich sequences have been shown to form four-stranded tetraplexes, and the implication of these structures in several biological roles has led to an increased interest in their physical properties. Tetraplexes may be important in the function of chromosome telomeres (Blackburn, 1991), the dimerization of human immunodefficiency virus RNA genome (Sundquist & Heaphy, 1993), and site specific recombination of immunoglobulin genes (Sen & Gilbert, 1988). The isolation of proteins that bind to and promote the formation of tetraplex structures also suggests the existence of a biological role for these structures (Fang & Cech, 1993). The telomeric sequences generally consist of several tandem repeats of guanine-rich sequences base-paired with a cytosine-rich strand. At the end of the chromosome, the guanine-rich strand extends beyond its complementary strand by 12−16 nucleotides (nt).[1] Oligodeoxyribonucleotides with telomeric sequences can form tetraplexes and are used as model systems for studying potential biological roles of these structures.

The structure and energetics of tetraplex structures have been investigated employing several physical techniques, including NMR (Aboul-ela *et al*., 1994), CD and Raman spectroscopy (Hardin *et al.*, 1992; Miura *et al*., 1995), calorimetry (Lu *et al*., 1993), mass spectroscopy (Goodlett *et al*., 1993), atomic force microscopy (Marsh *et al.*, 1995), and gel electrophoresis (Sen & Gilbert, 1990). A high-resolution crystal structure of a tetraplex formed by d(TGGGGT) in the presence of $Na^+$ has verified that the main structural motif of tetraplexes is a planar G quartet composed of four Hoogsteen base-paired guanines in a cyclical array (Laughlan *et al*., 1994). In addition to base stacking and hydrogen bonding, tetraplexes are stabilized by a cation positioned in the cavity between the planes of the tetrads which interacts with the eight surrounding guanine residues. The stabilizing ability of monovalent cations is ranked $K^+ > Rb^+ > Na^+ > Li^+ = Cs^+$, indicating that potassium ion has an optimum ionic radius for formation of the G tetraplex. Divalent cations are also capable of stabilizing G quartets: $Sr^{2+} > Ba^{2+} > Ca^{2+} > Mg^{2+}$ (Hardin *et al*., 1992; Venczel & Sen, 1993).

There are two principal types of known tetraplex structures. Tetraplexes arising from the interaction of four individual strands assume a conformation in which all four strands are parallel to each other (Laughlan *et al*., 1994; Aboul-ela *et al.*, 1994; Gupta *et al.*, 1993). There are also several possible

† This work was supported in part by a grant from the National Science and Engineering Research Council of Canada.

* Address correspondence to this author at Faculty of Pharmacy, University of Toronto, 19 Russell St., Toronto, Ontario M5S 2S2, Canada. Phone: (416) 978-7332. Fax: (416) 978-8511. E-mail: macgreg@phm.utoronto.ca.

[⊗] Abstract published in *Advance ACS Abstracts,* December 1, 1996.

[1] Abbreviations: CD, circular dichroism; EDTA, ethylenediaminetetraacetic acid; nt, nucleotide; ODN, oligodeoxyribonucleotide; Tris, tris(hydroxymethyl)aminomethane.

S0006-2960(96)00412-6 CCC: $12.00 

hairpin dimer structures that yield stable tetraplexes (Kang *et al.*, 1992; Smith & Feigon, 1993). The predominance of one conformation over the other is mostly dependent on the type of cation present. Sen and Gilbert (1990) have proposed that the structure adopted by the tetraplex-forming oligonucleotides is regulated by a sodium−potassium conformational switch. They demonstrated that the antiparallel bimolecular tetraplex predominates when the oligonucleotides are incubated in the presence of $K^+$; however, incubation in the presence of $Na^+$ leads to the formation of four-stranded complexes with parallel strand orientation. This phenomenon was explained by a kinetic effect. The faster-forming but energetically less favorable dimer is trapped by the high stabilizing ability of $K^+$, while treatment with $Na^+$ facilitates the association of parallel tetrads which are more stable but slower to form. The sodium−potassium switch, proposed by Sen and Gilbert (1990), is a good example of structural polymorphism. Miura *et al.* (1995) studied the effect of $Na^+$ and $K^+$ in stabilizing the quadruplex formation by $d(T_4G_4)_4$; this oligonucleotide can adopt a parallel four-stranded conformation or form a monomolecular, antiparallel fold-back quadruplex. Both sodium and potassium ions lead to formation of an antiparallel structure at low concentrations and facilitate the formation of a parallel tetraplex at high concentrations. However, $K^+$ is more effective than $Na^+$ at inducing the parallel association. The authors speculate that these cations may be important in the regulation of chromosomal association during meiosis by means of tetraplex formation by the G-rich overhang of telomeres.

There have been several reports of superstructures formed by G-rich oligomers. Sen and Gilbert (1992) reported that the oligodeoxyribonucleotides (ODNs) $d(T_9G_3)$ and $d(T_{12}G_3)$ assemble to form 4-, 8-, 12-, and 16-strand complexes in the presence of $K^+$. Tetraplexes formed by four strands of oligomer associate in a head-to-tail manner and are held together by a 3′ overhang of a single guanine. The thymines at the 5′ ends of these ODNs are displaced from the guanine helix. Recently, Marsh and Henderson (1994) reported that $d(G_4T_2G_4)$ spontaneously self-assembles into large superstructures that they called G-wires. These higher-order structures are resolved by gel electrophoresis as a ladder pattern. Once formed, G-wires are highly resistant to denaturation. These complexes have been visualized by atomic force microscopy (Marsh *et al.*, 1994) as rigid linear polymers with lengths varying from 10 to more than 1000 nm. It is interesting to note that the presence of magnesium and sodium ions gave rise to the most extensive polymerization.

Dai *et al.* (1995) studied the self-association of a series of ODNs containing one or two $G_4$ runs at their 3′ ends. Only those with two $G_4$ runs were able to self-assemble into high-molecular weight species, while the ODNs with one $G_4$ run existed as a duplexed hairpin and a four-stranded complex. Their results imply that the presence of at least two consecutive G-runs at the end of the ODN is crucial for its ability to associate into higher-order structures. The ODN $d(CGG)_4$ can form another class of supramolecular G quadruplex structures (Chen, 1995). These involve inter-tetraplex $C^+$·C base pairing, resulting in a dendrameric network of tetraplexes.

We report here that $d(A_{15}G_{15})$ is also able to self-assemble to form high-molecular weight oligomers and polymers. The structures formed are resistant to standard denaturation techniques and resolve as discrete bands on native and denaturing polyacrylamide electrophoresis gels. Partially complementary ODNs such as $dT_{10}$ and $d(CT_{15})$ interact with the oligomers formed by $d(A_{15}G_{15})$ without disrupting the distribution of the various oligomeric and polymeric structures. We hypothesize that these interactions arise through base pairing with the 5′ end of the $d(A_{15}G_{15})$ molecules in the complex. On the basis of these data, we propose a structural model for the higher-order complexes in which the monomers of $d(A_{15}G_{15})$ interact via formation of a tetraplex stem by the guanine residues. The adenine residues are single-stranded arms that project approximately radially from the guanine stem. Because of the disposition of the adenine residues, we refer to these structures as "frayed wires".

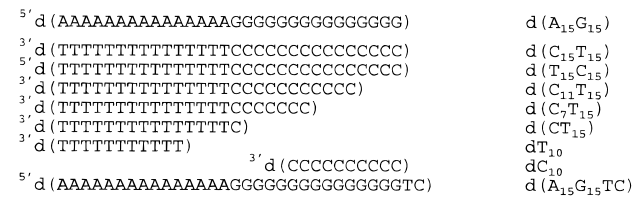


FIGURE 1: Synthetic oligodeoxyribonucleotides used in our experiments.

## MATERIALS AND METHODS

The sequences of the synthetic ODNs used in our experiments are presented in Figure 1. Lyophilized samples were diluted into 200 $\mu$L of deionized water. The concentrations of the ODNs in the resulting solutions were determined spectrophotometrically using the following extinction coefficients (in units of $M^{-1}$ $cm^{-1}$) for single strands at 260 nm calculated from the nearest-neighbor model (Cantor & Tinoco, 1965; Cantor *et al.*, 1970): $\epsilon[d(A_{15}G_{15})] = 3.341 \times 10^5$, $\epsilon[d(C_{15}T_{15})] = \epsilon[d(T_{15}C_{15})] = 2.661 \times 10^5$, $\epsilon[d(CT_{15})] = 1.169 \times 10^5$, $\epsilon[d(C_7T_{15})] = 1.601 \times 10^5$, $\epsilon[d(C_{11}T_{15})] = 1.887 \times 10^5$, $\epsilon[d(A_{15}G_{15}TC)] = 3.496 \times 10^5$, $\epsilon(dT_{10}) = 7.480 \times 10^4$, and $\epsilon(dC_{10}) = 7.220 \times 10^4$. Stock solutions of the ODNs at a concentration of 100 $\mu$M strands were prepared and stored at −20 °C.

*Higher-Order Complex Formation and Titration Experiments*. For all experiments, the same standard procedure was used for sample preparation unless stated otherwise. $d(A_{15}G_{15})$ (100 pmol) was 5′-end-labeled with T4 polynucleotide kinase and [$\gamma$-$^{32}$P]ATP in either 50 mM Tris-HCl (pH 7.5) containing 10 mM $MgCl_2$ or 10 mM Tris-acetate buffer (pH 7.0) containing 10 mM $MgCl_2$ and 50 mM KCl. Unincorporated $^{32}$P was removed from the solution by gel filtration chromatography. A typical reaction mixture with a total volume 10 $\mu$L was 2 $\mu$M in strands of unlabeled $d(A_{15}G_{15})$ oligonucleotide, approximately 10 nM $^{32}$P-labeled $d(A_{15}G_{15})$, 90 mM Tris-borate, and 5 mM $MgCl_2$ (TBM). The tubes containing the samples were placed in a 1 L bath of boiling water, and the bath was removed from the heat and allowed to cool overnight to 10 °C. For analysis under denaturing conditions, 3 $\mu$L of the sample was diluted with 3 $\mu$L of formamide loading buffer, heated to 95 °C, and run through a 10% polyacrylamide gel containing 7 M urea at 55 °C. Mobility shift experiments were carried out with 6 $\mu$L of the sample diluted with 3 $\mu$L of a 20% sucrose solution in TBM. The 10% polyacrylamide gels were run at 10 °C. TBM or TBE (90 mM Tris-borate and 2 mM EDTA) was

used as a running buffer. All gels were dried under vacuum at 80 °C. The pattern of bands was visualized using an Ambis model 4000 radioanalytic imaging system. We followed the same procedure for titration experiments, but the concentration of unlabeled d($A_{15}G_{15}$) was varied from 0.01 to 20 $\mu$M.

*Interaction of Complementary Strands with the Polymer.* The samples of d($A_{15}G_{15}$) oligomer were prepared as described above. After annealing, a solution of one of the complementary strands was added to the mixture. The sample was allowed to equilibrate for 3 h at 10 °C. Prior to being loaded on a nondenaturing polyacrylamide gel, the samples were diluted with 2 $\mu$L of a 40% sucrose solution in water. TBE was used as a running buffer for electrophoresis. Depending on the type of experiment, we used either labeled d($A_{15}G_{15}$) oligomer or $^{32}$P-labeled complementary strand.

*Mung Bean Nuclease Assay.* Samples were prepared in 10 mM 1,3-bis[tris(hydroxymethyl)methylamino]propane hydrochloride (pH 7.0 at 25 °C) containing 10 mM $MgCl_2$, 1 mM dithiothreitol, and 1 mM $ZnSO_4$. Mung bean nuclease (2 $\mu$L, 15 600 units/mL) was added to 45 $\mu$L of the sample and incubated at 30 °C. Aliquots (5 $\mu$L) were removed from the reaction mixture at various times. The digestion was stopped by addition of 5 $\mu$L of formamide loading buffer containing 50 mM EDTA.

*Effect of Mono- and Divalent Cations on the Formation of Complexes.* The samples were prepared in 10 mM Tris-borate buffer containing 50 mM XCl (X = Na, K, or $NH_4$) or 5 mM $MgCl_2$.

## RESULTS

*Higher-Order Complex Formation.* As shown in lanes 1−5 of Figure 2a, d($A_{15}G_{15}$) readily self-assembles into stable higher-order complexes in the presence of 5 mM $MgCl_2$. The regular pattern of nine or more discrete bands observed on a denaturing gel demonstrates that these complexes are resistant to standard DNA denaturation conditions. A similar pattern of bands is also observed on native gels (Figure 2b, lanes 1−5). The band with the highest mobility corresponds to the single d($A_{15}G_{15}$) oligomer. Plotting the logarithm of mobilities of the most intense bands (labeled 2, 3, etc., in Figure 2a,b) versus the band number resulted in straight lines with correlation coefficients greater than 0.99 (Figure 3). This suggests that the complexes which appear on the gel as bands with the lower mobility have similar structures with respect to shape, charge density, flexibility, etc., but that they differ in the number of associated strands, i.e. the molecular weight. The gel electrophoresis patterns suggest that the polymerization occurs by the successive addition of a parent d($A_{15}G_{15}$) oligomer to initially formed complexes. Band 1 (monomer) has a somewhat higher mobility than expected, indicating that its structure is different. This effect is due to the higher flexibility and a lower cross section of the single strands relative to those of the multistranded complexes.

Titration experiments performed over a wide range of concentrations of the d($A_{15}G_{15}$) oligomer reveal the dependence of the fraction of the high-molecular weight species (polymer) on the concentration of d($A_{15}G_{15}$). In Figure 4, histograms of two lanes of the nondenaturing gel illustrate that increasing the concentration of d($A_{15}G_{15}$) favors the formation of polymers at the expense of lower-molecular

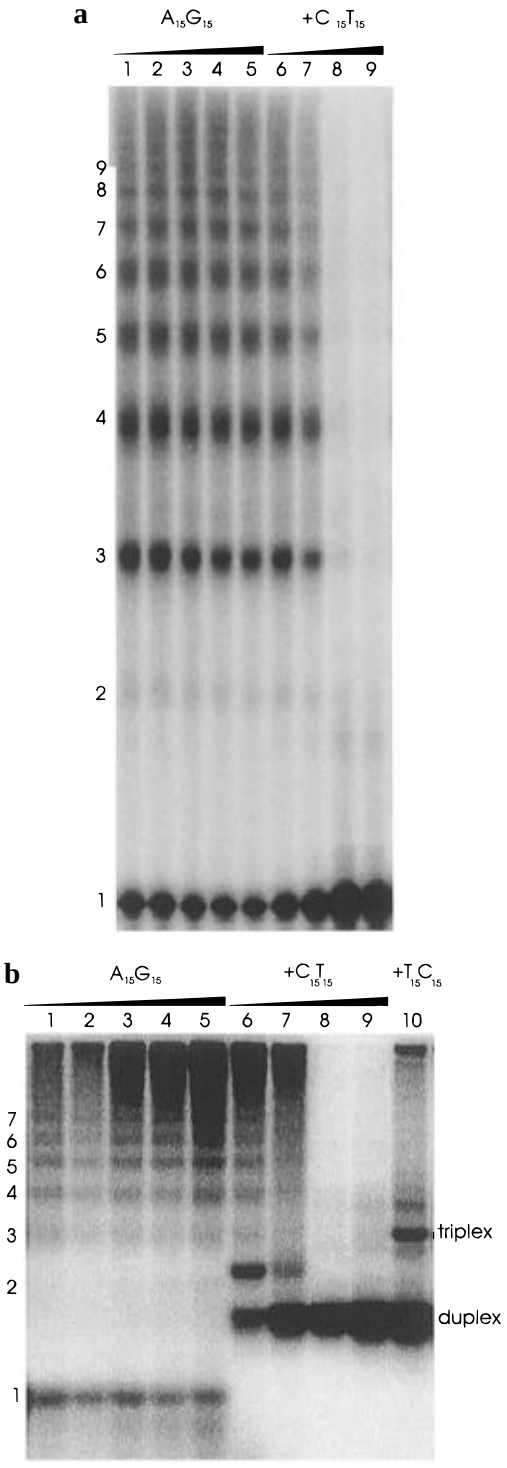


FIGURE 2: (a) Self-assembly of the d($A_{15}G_{15}$) oligomer into high-molecular weight complexes resolved on 10% denaturing polyacrylamide gel (7 M urea, electrophoresis carried out at 55 °C). Lanes 1−5, the effect of d($A_{15}G_{15}$) concentration on aggregation: 0.5, 1, 2, 4, and 7 $\mu$M d($A_{15}G_{15}$) strands, respectively. Lanes 6−9, annealing of solutions containing 0.5, 1, 2, and 4 $\mu$M concentrations, respectively, of the fully complementary strand d($C_{15}T_{15}$) with 2 $\mu$M d($A_{15}G_{15}$). (b) Self-assembly of d($A_{15}G_{15}$) into high-molecular weight complexes resolved on 10% native polyacrylamide gel and TBM running buffer. Lanes 1−5, the effect of d($A_{15}G_{15}$) concentration on aggregation: 0.5, 1, 2, 4, and 7 $\mu$M d($A_{15}G_{15}$) strand concentration, respectively. Lanes 6−9, annealing of solutions containing 0.5, 1, 2, and 4 $\mu$M concentrations, respectively, of the fully complementary strand d($C_{15}T_{15}$) with 2 $\mu$M d($A_{15}G_{15}$). Lane 10 shows the formation of a triple-stranded species upon addition of the third strand d($T_{15}C_{15}$) to the solution containing duplex (lane 7).

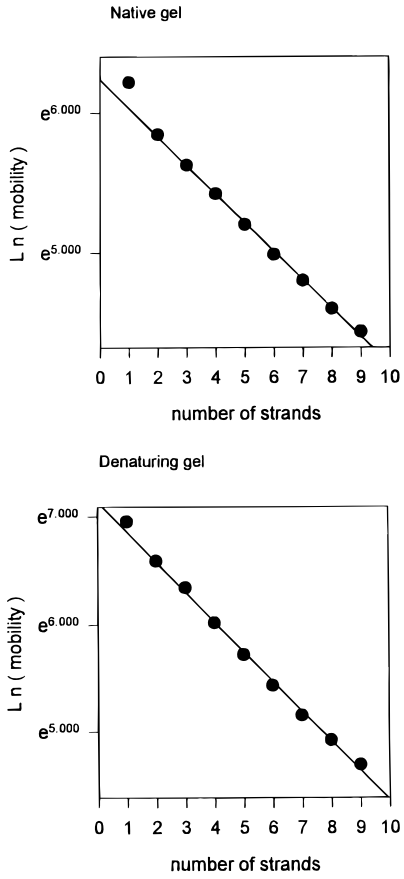


FIGURE 3: Semilogarithmic plots of the mobilities (distance migrated on the gel) of the bands versus the band numbers for native and denaturing polyacrylamide gels (see Figure 2a,b). The solid lines are linear least-squares fits of all the data except the first point ($r^2 > 0.99$).

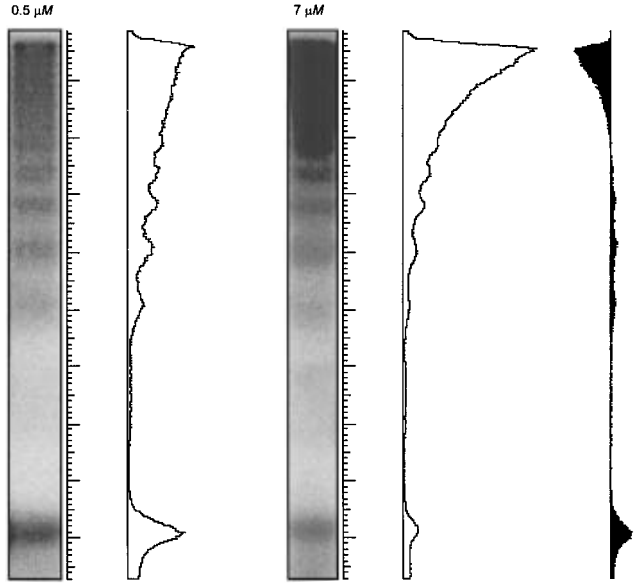


FIGURE 4: Histograms of the band intensities at different concentrations of $d(A_{15}G_{15})$ resolved on a native polyacrylamide gel. The concentrations are shown at the top of each lane. The difference between the two histogram plots is shown at the far right.

weight species. The intensity of the band corresponding to the monomer decreases, while the top portion of the gel becomes more intense. The same effect can be observed on denaturing gel (data not shown), where a redistribution of labeled $d(A_{15}G_{15})$ strands between the lower- and higher-

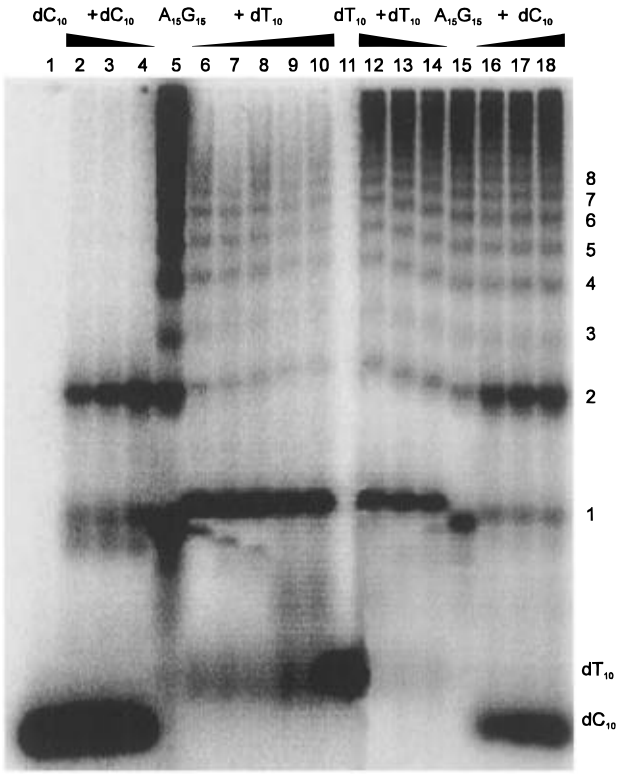


FIGURE 5: Annealing of $d(A_{15}G_{15})$ with $dT_{10}$ and $dC_{10}$ as resolved by native gel electrophoresis. All samples contained 2 $\mu$M $d(A_{15}G_{15})$ oligomer. The concentration of $dC_{10}$ and $dT_{10}$ ranged from 0.1 to 2 $\mu$M. The gradients at the top of some lanes are intended to show the increasing concentration of $dT_{10}$ or $dC_{10}$. Lanes 1−4, $^{32}$P-labeled $dC_{10}$. Lanes 16−18, both $d(A_{15}G_{15})$ and $dC_{10}$ $^{32}$P-labeled. Lanes 6−10, $^{32}$P-labeled $dT_{10}$. Lanes 12−14, both $d(A_{15}G_{15})$ and $dT_{10}$ $^{32}$P-labeled. Lanes 5 and 15 are controls, with only $^{32}$P-labeled $d(A_{15}G_{15})$ present in solution. Lanes 1 and 11 contained only $^{32}$P-labeled $dC_{10}$ or $dT_{10}$, as indicated.

molecular weight species occurs in favor of the polymer. A clear tendency toward polymerization with an increase in the total concentration of the oligomer is consistent with a mechanism in which the polymeric aggregates form by consecutive addition of $d(A_{15}G_{15})$ monomers to the other species present in solution (dimers, trimers, tetramers, etc.).

*Enzymatic Degradation by Mung Bean Nuclease.* Mung bean nuclease, a single-strand specific endonuclease, was used to determine the accessibility of the labeled 5′ end of the polymers. This enzyme readily cuts a six-nucleotide fragment from 5′ end (A-tail) of all of the species, implying that the 5′ end A-tail is not engaged in stable interactions with the rest of the polymer structure. However, the absence of smearing of bands even in the lanes corresponding to long digestion times suggests that the 3′ end G-run remains protected from the action of this nuclease, presumably due to the formation of tetraplex structures.

*Interaction of $d(A_{15}G_{15})$ Polymers with Complementary Strands.* We used $dT_{10}$ and $dC_{10}$ to probe the ability of the polymerized structures to form Watson−Crick duplexes with $d(A_{15}G_{15})$. Under nondenaturing conditions, when $^{32}$P-labeled $dC_{10}$ is incubated with $d(A_{15}G_{15})$, two distinct bands are observed (Figure 5, lanes 2−4). These correspond to $dC_{10}$ complexed to single-stranded $d(A_{15}G_{15})$ and to its dimer conformation. There are no bands representing species with higher molecular weights. Apparently, base pairing of $dC_{10}$ with the guanine tracts of $d(A_{15}G_{15})$ strands comprising the polymer is not possible because they are already engaged in

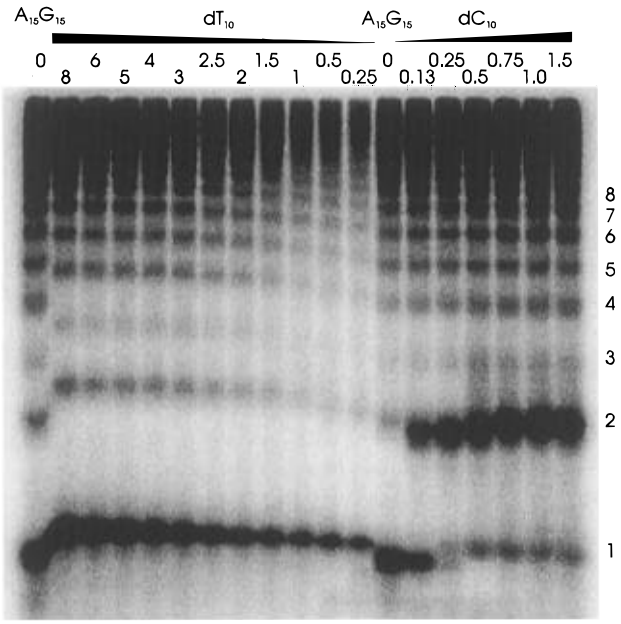


FIGURE 6: Mobility of $^{32}$P-labeled d($A_{15}G_{15}$) on a native gel after annealing with a wide concentration range of $dT_{10}$ and $dC_{10}$. The concentration of d($A_{15}G_{15}$) is 2 $\mu$M in all samples, and the concentration of $dT_{10}$ or $dC_{10}$ (in micromolar) is shown at the top of each lane.

G-tetrad interactions. It is interesting that the distribution of species between the first (monomer) and the second (dimer) bands shifts in favor of the dimer when $dC_{10}$ is added to labeled d($A_{15}G_{15}$) (lanes 16−18). $dC_{10}$ facilitates the formation of aggregates that migrate at the same position as d($A_{15}G_{15}$) dimers, possibly involving structures that are substantially different from those formed by d($A_{15}G_{15}$) alone. We are continuing a more detailed investigation of the composition and structure of these species; however, their characterization is not the aim of this report. The magnitude of the shift of the fastest-migrating band (band 1) toward a higher molecular weight is consistent with the addition of 10 nt ($dC_{10}$) to the single strand. The mobility shift of the second band is small and in the opposite direction, again suggesting the existence of complexes with strand arrangements that differ from that expected of the d($A_{15}G_{15}$) dimer.

Figure 5 shows that after incubation of d($A_{15}G_{15}$) with $^{32}$P-labeled $dT_{10}$ electrophoresis on a native gel yields a pattern of bands that is similar to that of d($A_{15}G_{15}$) oligomer alone (lanes 6−10); however, there is a mobility shift toward higher molecular weights for all the bands. The lower the mobility of the species in the absence of $dT_{10}$, the more it shifts (on a logarithmic scale) when the concentration of $dT_{10}$ increases (Figure 6). Thus, the complexes with higher molecular weights, which consist of more strands of d($A_{15}G_{15}$), have more binding sites for $dT_{10}$. The mobility, i.e. the molecular weight of the d($A_{15}G_{15}$)−$dT_{10}$ complexes, does not change further after an equimolar concentration of $dT_{10}$ has been added to the solution of d($A_{15}G_{15}$). The data in Figure 6 also allow us to infer that the binding of $dT_{10}$ does not significantly alter the relative stability of the different polymeric species because, to a first approximation, the distribution of these species is unaffected by the addition of this ODN.

The most striking characteristic of the polymeric complexes formed by d($A_{15}G_{15}$) is their resistance to denaturation. However, annealing d($A_{15}G_{15}$) with increasing concentrations of the complementary ODN, d($C_{15}T_{15}$), leads to the disappearance of the bands arising from the high-molecular weight species and the appearance of a single band corresponding to the Watson−Crick duplex (Figure 2b, lanes 6−9). The d($A_{15}G_{15}$) polymers are also eliminated following a 3 h incubation in the presence of the complementary strand at 22 °C (Figure 7, lane 2). High-molecular weight species are present in trace amounts. Evidently, the presence of d($C_{15}T_{15}$) destabilizes the polymer and causes it to degrade and form duplex DNA. As expected, annealing the Watson−Crick duplex with the third strand, d($T_{15}C_{15}$), results in formation of triple-stranded DNA, which is resolved by gel electrophoresis as a band with lower mobility than that of a duplex (Figure 2b, lane 10). The duplex DNA structures are readily denatured, and on a denaturing gel, one observes only a single band corresponding to single-stranded d($A_{15}G_{15}$) (Figure 2b, lanes 8 and 9).

Given that $dT_{10}$ does not interfere with polymerization of d($A_{15}G_{15}$), and d($C_{15}T_{15}$) completely abolishes polymerization, it is interesting to consider the minimum length of the C-run of the complementary strand which would destabilize the polymer complexes. We performed a series of experiments with the ODNs d($C_nT_{15}$), where $n = 1$, 7, 11, or 15. The electrophoresis patterns obtained on a native gel after incubation of d($A_{15}G_{15}$) polymers with these ODNs are shown in Figure 7. The band with the highest mobility in each lane corresponds to the Watson−Crick duplex formed by the interaction between a d($A_{15}G_{15}$) monomer and one strand of d($C_nT_{15}$). The difference in mobilities of the duplexes is consistent with the change in molecular weights; for example, the d($A_{15}G_{15}$)·d($C_{15}T_{15}$) duplex migrates slower than d($A_{15}G_{15}$)·d($CT_{15}$) (lanes 2 and 8).

When the d($C_nT_{15}$) ODNs are present at lower concentrations than d($A_{15}G_{15}$) (Figure 7, lanes 3, 5, 7, and 9), the pattern of slow-migrating bands resembles that of the d($A_{15}G_{15}$) polymers (lanes 1 and 10); however, the intensity is lower, and the bands are somewhat smeared. Increasing the concentration of d($C_nT_{15}$) leads to the formation of well-defined bands near the top of the gel for d($CT_{15}$) and d($C_7T_{15}$) (lanes 8 and 6), while the polymer bands disappear in the presence of d($C_{11}T_{15}$) and d($C_{15}T_{15}$) (lanes 4 and 2). We propose that this behavior arises from the formation of standard duplex structures between d($CT_{15}$) or d($C_7T_{15}$) and the adenines of the d($A_{15}G_{15}$) polymers. This is similar to what we observed when $dT_{10}$ was annealed to d($A_{15}G_{15}$). In addition, the mobility shifts of the individual bands are consistent with the expected increase of the molecular weights of the species after addition of the corresponding number of the d($C_nT_{15}$) strands. For example, band 4 in lane 8 (indicated by the arrow) corresponds to species formed by the interaction of four molecules of d($CT_{15}$) with a four-stranded complex of d($A_{15}G_{15}$), bringing the total molecular weight close to that of the d($A_{15}G_{15}$) complex composed of six strands (lane 10, band 6).

Incubation of the d($A_{15}G_{15}$) polymers with d($C_{11}T_{15}$) or d($C_{15}T_{15}$) results in a loss of the bands corresponding to the higher-molecular weight complexes, indicating disruption of the polymeric complexes. Evidently, aggregation of d($A_{15}G_{15}$) to form polymers is energetically more favorable than duplex formation up to a certain length of the 3′ G-overhang. Under the conditions of our experiments, the minimum number of unpaired gaunosines capable of stabilizing polymerized d($A_{15}G_{15}$) complexes is more than four and less than eight.

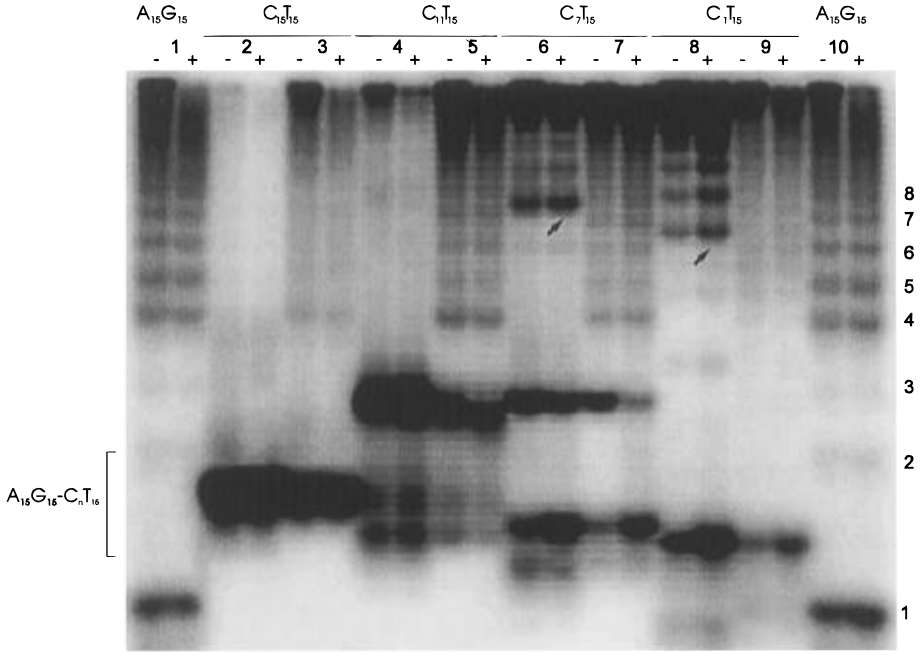


FIGURE 7: Annealing of $^{32}$P-labeled d($A_{15}G_{15}$) with d($C_nT_{15}$) ($n$ = 1, 7, 11, and 15) resolved by native gel electrophoresis. All samples were 2 $\mu$M in d($A_{15}G_{15}$); the concentration of the complementary strands was either 1 $\mu$M (lanes 3, 5, 7, and 9) or 4 $\mu$M (lanes 2, 4, 6, and 8). The lanes are presented as pairs; for each pair, the sample loaded in the lane marked − was kept at 10 °C. The samples loaded in the lanes marked + were heated to 100 °C and then allowed to cool slowly to 10 °C prior to loading. The arrows in lanes 6 and 8 indicate the position of the complexes consisting of four d($A_{15}G_{15}$) strands after interaction with d($C_{11}T_{15}$) and d($C_7T_{15}$), respectively. Lanes 1 and 10 are controls with no d($C_nT_{15}$) added.

Interestingly, the interaction between d($A_{15}G_{15}$) and the intermediate length complementary ODNs, d($C_7T_{15}$) and d($C_{11}T_{15}$), leads to the appearance of an intense band that migrates slower than d($A_{15}G_{15}$)·d($C_nT_{15}$) complexes (Figure 7, lanes 4−7). Perhaps the formation of these species is driven by the same mechanism as redistribution of d($A_{15}G_{15}$) strands following addition of $dC_{10}$. Apparently, the presence of ODNs containing long cytosine runs favors dimerization at the expense of the monomeric species.

*Complex Formation by a d(A15G15TC) Oligomer*. To assess the role that the 3′ end plays in complex formation, we added two nucleotides, dTC, to the 3′ end of d($A_{15}G_{15}$). We found that under the same experimental conditions the pattern of bands for d($A_{15}G_{15}$TC) does not show evidence of formation of polymers (data not shown). The addition of the non-guanine nucleotides to the 3′ end of the oligomer inhibits the formation of high-molecular weight species, while the formation of dimers and complexes consisting of three and four strands is enhanced.

*Effect of Cations on Polymerization*. The type and concentration of the cation present in the solution play important roles in determining the conformation adopted by the oligomer. The pattern of bands of the samples prepared in the presence of different cations is presented in Figure 8. Monovalent cations ($Na^+$, $K^+$, and $NH_4^+$) stabilize complexes consisting of four, five, and six strands of d($A_{15}G_{15}$), but they do not lead to the formation of higher-molecular weight species. The distribution between different complexes (monomer, dimer, trimer, etc.) is determined by not only the type of cation but also its concentration. For example, 5 mM $Na^+$ leads to the formation of a very intense band that we attribute to a two-stranded d($A_{15}G_{15}$) hairpin tetraplex. Increasing the $Na^+$ concentration to 100 mM shifts the equilibrium even further toward dimer, and there is no monomer remaining. The split of band 2 at high concentrations of $Na^+$ indicates that there are two types of two-stranded hairpin tetraplexes that can be resolved on these gels. The two simplest possibilities are dimer hairpins with the 5′ adenines at either the same or opposite ends of the structure.

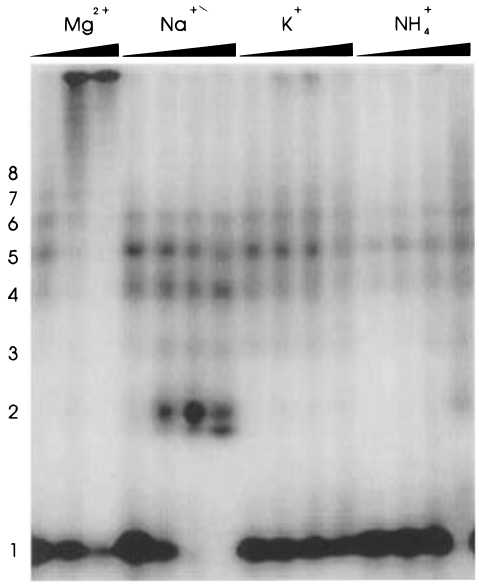


FIGURE 8: Effect of the type and concentration of cations on polymer formation resolved by native gel electrophoresis. The concentration of cations increases from left to right: 1, 5, and 20 mM for $Mg^{2+}$ and 1, 5, 20, and 100 mM for $Na^+$, $K^+$, and $NH_4^+$.

The pattern observed for samples prepared in solutions containing divalent cations is quite different. In buffer solutions containing $Mg^{2+}$, d($A_{15}G_{15}$) has a clear tendency toward polymerization at the expense of the lower-molecular weight species. An increase in the concentration of the

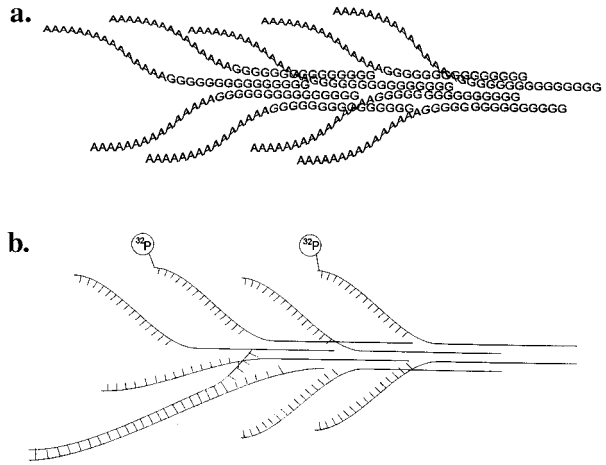


FIGURE 9: (a) Frayed wires. A model of the polymer formed by d($A_{15}G_{15}$). The complexes have two distinct structural regions, a stem made up of G tetrads and single-stranded adenine arms projecting from the stem. The extreme stability of these structures results from the large number of G-tetrads in the stem. The adenosine residues at the 5′ end of d($A_{15}G_{15}$) frayed wires are presumably unstructured. (b) A model for disruption of the complexes through interactions with the complementary strand. Initial interactions lead to base pair formation between the arms of the frayed wire and the thymines of the complementary strand. The duplex propagates into the stem region, destabilizing the G-tetraplex and leading to strands being either partially or fully peeled away from the frayed wire. The extent of the removal of a d($A_{15}G_{15}$) strand depends upon the length of the complementary ODN.

cation promotes the formation of the polymer with higher molecular weights.

## DISCUSSION

On the basis of the results of the experiments described above, we propose the model of the high-molecular weight polymeric complexes formed by d($A_{15}G_{15}$) presented in Figure 9a,b. In our model, these complexes consist of two distinct structural regions: a stem made up of G tetrads and single-stranded adenine arms projecting radially from the stem. The extreme stability of the polymer is a result of the large number of G-tetrads in the stem. In the polymeric complexes, the adenine residues at the 5′ end of d($A_{15}G_{15}$) are presumably rather unstructured. To emphasize the proposed displacement of the adenosine arms from the putative tetraplex stem and to distinguish these structures from G-wires, introduced by Marsh and Henderson (1994), we call the polymers formed by d($A_{15}G_{15}$) frayed wires. The structure shown is intended to provide a conceptual model of the species formed by d($A_{15}G_{15}$) and does not represent any particular structure in detail. One feature missing from Figure 9a,b is the interactions at the end of the stems. The stems are likely terminated by hairpins; however, this detail has been omitted because of the low level of our present understanding of these structures. Our data show that stable frayed wires form only when there are between four and eight guanosine residues at the 3′ end of the ODN. This is consistent with the ability of d($G_4T_2G_4$) to form G-wires.

There are three details in which our findings differ significantly from those of Marsh and Henderson (1994). First, they found that addition of a phosphate group to the 5′ end of their ODN abolished its ability to form G-wires. The ODN used in our study has 15 adenine residues at the 5′ end and yet yields stable polymer structures. The fact that the ODN we used, d($A_{15}G_{15}$), has up to 15 guanine tetrads in the stem may account for this difference.

The second distinction between the properties of G-wires and frayed wires is the salt dependence of the stabilization of the polymer structures (Figure 8). We found that sodium, potassium, and ammonium ions stabilize oligomerization of d($A_{15}G_{15}$) but only a limited amount of polymerization. Among these monovalent ions, we found that sodium stabilized oligomerization the most, with potassium and ammonium being approximately equal in their ability to oligomerize. In contrast to this, G-wires are more stable in the presence of potassium ions than in sodium ions. The most extensive polymerization was observed in solutions containing magnesium ions. Similar behavior was reported in the studies of Marsh *et al*. (1994) and Dai *et al*. (1995). Again, it seems reasonable that the larger number of guanine residues in the stem may be responsible for different salt dependencies of G-wires and frayed wires.

The third difference between the structures of frayed wires and G-wires is the way the monomers interact to form polymers. In our proposed structure, the monomers of d($A_{15}G_{15}$) add to overhangs in the tetraplex stem region of the initially formed aggregates. The tetraplex motif that stabilizes G-wires is presumed to arise from the interaction between two pairs of d($G_4T_2G_4$) molecules. Units of tetraplex structure are joined together by bridges made up of the two central thymine residues. For our sequence, we believe that the structure put forth in Figure 9a,b is consistent with the electrophoretic mobility of the slow-migrating bands. Because of the sequence difference, it seems entirely possible that the ODN used by Marsh and Henderson might adopt a structure dissimilar to the one we propose.

The unique feature of the high-molecular weight species formed by d($A_{15}G_{15}$) is the ability of the arms to form sequence specific interactions with complementary ODNs (Figure 9b). The structure proposed by Sen and Gilbert (1992) for oligomers of d($T_9G_3$) and d($T_{12}G_3$) also included arms; however, they did not demonstrate that the arms were capable of forming interactions with other ODNs. In addition, because the stem of their ODNs contained only three guanine residues, the structures presumably would be denatured by standard procedures.

In our model, the stem region cannot form stable complexes with $dC_{10}$ because of the involvement of the guanine residues of polymerized d($A_{15}G_{15}$) species in G-tetrads. We hypothesize that the ability of the fully complementary strand, d($C_{15}T_{15}$), to destabilize d($A_{15}G_{15}$) polymers is initiated through the formation of base-pairing interactions involving only the arms (Figure 9b). After formation of a stable nucleation complex between the arms and the thymine residues of the complementary strand, base pairing then propagates in the 5′ direction of d($C_{15}T_{15}$) into the stem region. In this way, strands of d($A_{15}G_{15}$) are peeled off the polymer structure. The fact that the duplexes formed this way can be denatured by standard techniques is evidence of a subtle balance of thermodynamic and kinetic effects in the formation and stabilization of frayed wires.

## REFERENCES

Aboul-ela, F., Murchie, A. I. H., Norman, D. G., & Lilley, D. M. J. (1994) *J. Mol. Biol. 243*, 458−471.
Blackburn, E. H. (1991) *Nature 350*, 569−573.
Cantor, C. R., & Tinoco, I., Jr. (1965) *J. Mol. Biol. 13*, 65−77.

Cantor, C. R., Warshaw, M. M., & Herman, S. (1970) *Biopolymers 9*, 1059−1077.
Chen, F.-M. (1995) *J. Biol. Chem. 270*, 23090−23096.
Dai, T.-Y., Marotta, S. P., & Sheardy, R. D. (1995) *Biochemistry 34*, 3655−3662.
Fang, G. W., & Cech, T. R. (1993) *Cell 74*, 875−885.
Goodlett, D. R., Camp, D. G., Hardin, C. C., Corregan, M., & Smith, R. D. (1993) *Biol. Mass Spectrom. 22*, 181−183.
Gupta, G., Garcia, A. E., Guo, Q., Lu, M., & Kallenbach, N. R. (1993) *Biochemistry 32*, 7098−7103.
Hardin, C. C., Watson, T., Corregan, M., & Bailey, C. (1992) *Biochemistry 31*, 833−841.
Kang, C., Zhang, X., Ratliff, R., Moyzis, R., & Rich, A. (1992) *Nature 356*, 126−131.
Laughlan, G., Murchie, A. I. H., Norman, D. G., Moore, M. H., Moody, P. C. E., Lilley, D. M. J., & Luisi, B. (1994) *Science 265*, 520−524.
Lu, M., Guo, Q., & Kallenbach, N. R. (1993) *Biochemistry 32*, 598−601.
Marsh, T. C., & Henderson, E. (1994) *Biochemistry 33*, 10718−10724.
Marsh, T. C., Vesenka, J., & Henderson, E. (1994) *Nucleic Acids Res. 23*, 696−700.
Miura, T., Benevides, J. M., & Thomas, G. J. (1995) *J. Mol. Biol. 248*, 233−238.
Sen, D., & Gilbert, W. (1988) *Nature 334*, 364−366.
Sen, D., & Gilbert, W. (1990) *Nature 344*, 410−414.
Sen, D., & Gilbert, W. (1992) *Biochemistry 31*, 65−70.
Smith, F. W., & Feigon, J. (1993) *Biochemistry 32*, 8682−8692.
Sundquist, W. I., & Heaphy, S. (1993) *Proc. Natl. Acad. Sci. U.S.A. 90*, 3393−3397.
Venczel, E. A., & Sen, D. (1993) *Biochemistry 32*, 6220−6228.

BI960412D